



# Dectin-2-Targeted Antifungal Liposomes Exhibit Enhanced Efficacy

Suresh Ambati,<sup>a</sup> Emma C. Ellis,<sup>a</sup> Jianfeng Lin,<sup>b</sup>  Xiaorong Lin,<sup>b</sup> Zachary A. Lewis,<sup>b</sup> Richard B. Meagher<sup>a</sup>

<sup>a</sup>Department of Genetics, University of Georgia, Athens, Georgia, USA

<sup>b</sup>Department of Microbiology, University of Georgia, Athens, Georgia, USA

**ABSTRACT** *Candida albicans*, *Cryptococcus neoformans*, and *Aspergillus fumigatus* cause life-threatening candidiasis, cryptococcosis, and aspergillosis, resulting in several hundred thousand deaths annually. The patients at the greatest risk of developing these life-threatening invasive fungal infections have weakened immune systems. The vulnerable population is increasing due to rising numbers of immunocompromised individuals as a result of HIV infection or immunosuppressed individuals receiving anticancer therapies and/or stem cell or organ transplants. While patients are treated with antifungals such as amphotericin B, all antifungals have serious limitations due to lack of sufficient fungicidal effect and/or host toxicity. Even with treatment, 1-year survival rates are low. We explored methods of increasing drug effectiveness by designing fungicide-loaded liposomes specifically targeted to fungal cells. Most pathogenic fungi are encased in cell walls and exopolysaccharide matrices rich in mannans. Dectin-2 is a mammalian innate immune membrane receptor that binds as a dimer to mannans and signals fungal infection. We coated amphotericin-loaded liposomes with monomers of Dectin-2's mannan-binding domain, sDectin-2. sDectin monomers were free to float in the lipid membrane and form dimers that bind mannan substrates. sDectin-2-coated liposomes bound orders of magnitude more efficiently to the extracellular matrices of several developmental stages of *C. albicans*, *C. neoformans*, and *A. fumigatus* than untargeted control liposomes. Dectin-2-coated amphotericin B-loaded liposomes reduced the growth and viability of all three species more than an order of magnitude more efficiently than untargeted control liposomes and dramatically decreased the effective dose. Future efforts focus on examining pan-antifungal targeted liposomal drugs in animal models of fungal diseases.

**IMPORTANCE** Invasive fungal diseases caused by *Candida albicans*, *Cryptococcus neoformans*, and *Aspergillus fumigatus* have mortality rates ranging from 10 to 95%. Individual patient costs may exceed \$100,000 in the United States. All antifungals in current use have serious limitations due to host toxicity and/or insufficient fungal cell killing that results in recurrent infections. Few new antifungal drugs have been introduced in the last 2 decades. Hence, there is a critical need for improved antifungal therapeutics. By targeting antifungal-loaded liposomes to  $\alpha$ -mannans in the extracellular matrices secreted by these fungi, we dramatically reduced the effective dose of drug. Dectin-2-coated liposomes loaded with amphotericin B bound 50- to 150-fold more strongly to *C. albicans*, *C. neoformans*, and *A. fumigatus* than untargeted liposomes and killed these fungi more than an order of magnitude more efficiently. Targeting drug-loaded liposomes specifically to fungal cells has the potential to greatly enhance the efficacy of most antifungal drugs.

**KEYWORDS** liposomes, Dectin-2, exopolysaccharide matrix, mannan, amphotericin B, invasive fungal disease

**Citation** Ambati S, Ellis EC, Lin J, Lin X, Lewis ZA, Meagher RB. 2019. Dectin-2-targeted antifungal liposomes exhibit enhanced efficacy. mSphere 4:e00715-19. <https://doi.org/10.1128/mSphere.00715-19>.

**Editor** J. Andrew Alspaugh, Duke University Medical Center

**Copyright** © 2019 Ambati et al. This is an open-access article distributed under the terms of the [Creative Commons Attribution 4.0 International license](https://creativecommons.org/licenses/by/4.0/).

Address correspondence to Richard B. Meagher, [meagher@uga.edu](mailto:meagher@uga.edu).

 We targeted antifungal drug-loaded liposomes specifically to fungal cells thereby decreasing the effective antifungal dose more than an order of magnitude.

**Received** 28 September 2019

**Accepted** 9 October 2019

**Published** 30 October 2019

*Candida albicans* is a commensal fungus found on the skin and in the intestinal track, while *Cryptococcus neoformans* and *Aspergillus fumigatus* are indigenous to soil. Candidiasis, cryptococcal meningitis, and pulmonary aspergillosis claim more than one million lives annually (1–5). Health care costs in the United States for these three invasive fungal diseases exceed 4.7 billion dollars annually (6). Patients at the greatest risk of developing life-threatening fungal infections include those with weakened immune systems and/or various lung diseases, such as immunosuppressed and immunocompromised individuals, patients receiving long-term treatment for inflammatory diseases, and AIDS patients. Furthermore, the number of immunocompromised individuals, who are susceptible to these opportunistic fungal infections, is increasing due to growing numbers of patients on immunosuppressants as part of their therapy for cancer, for stem cell and organ transplants, and for inflammatory diseases (3, 7).

Patients with candidiasis, cryptococcosis, or aspergillosis are treated with antifungals such as the fungicidal polyene amphotericin B (AmB) and/or other fungicides. However, even with antifungal therapies, there are alarmingly high mortality rates that range from 10% to 95%, depending upon the patient population and particular fungal infection (1–5, 8, 9). Furthermore, all known synthetic antifungal agents such as AmB are toxic to human cells and organs. For example, AmB treatment frequently causes renal toxicity that is often fatal (10–12), and diverse prophylactic strategies are employed to reduce adverse outcomes for patients (13). The incidence of antifungal-resistant *Cryptococcus* and *Candida species* is increasing (14–18). There are few new antifungal drugs in play (19). Of the ten antifungals listed by the CDC (2) as commonly employed to treat these diseases, only isavuconazole was introduced in the last 2 decades (20, 21). Clearly, there is a need for new antifungal therapeutic treatments with improved efficacy.

Since the 1980s, antibodies have been used to target anticancer drug-loaded liposomes to cancer cells with demonstrated improvements in therapeutic efficiency (22, 23). Antibody-coated immunoliposomes target the delivery of bundled anticancer drugs specifically to tumors or dispersed cancer cells compared to the passive delivery of drugs to all organs and cells by untargeted drug-loaded liposomes or free drug. Antibody-targeted drug-loaded liposomes generally increase cell-type specificity and reduce host cytotoxicity by 5- to 10-fold over passive delivery (24–26). Several targeted liposomal drugs have been FDA approved (27–31). Our goal has been to target antifungals packaged in liposomes specifically to fungal cells. The pharmacokinetic concept behind the improved performance of targeted liposomes is that by maintaining high drug concentration in the cell vicinity, the efficacy of drug delivery is increased, while the dose delivered to the patient is reduced, and hence, host toxicity is reduced.

As with many pathogenic fungi, the outer layer of the cell walls and extracellular matrices of *C. albicans*, *C. neoformans*, and *A. fumigatus* and the extracellular capsule of *C. neoformans* contain mannan-rich polysaccharides and mannoproteins. Their extracellular matrices are essential for these pathogenic fungal cells to adhere to host cell and organ surfaces and to implanted medical devices (32–36) and confer increased resistance to antifungals (37, 38). Hence, the extracellular matrix contributes to poor clinical outcomes (33, 34, 39–41). Herein, we sought to target fungicide-loaded liposomes specifically to mannans, thereby increasing drug concentration at or near to the fungal cell surface and improving antifungal therapeutic efficiency.

Dectin-2 is encoded by the human and mouse C-type LECTin receptor gene *CLEC6A*. Dectin-2 binds  $\alpha$ -mannans and N-linked and O-linked mannans in mannoproteins (42–46). Dectin-2 is expressed in the plasma membrane of some lymphocytes, with its mannan binding domain (sDectin-2) on the outside of these cells and its signaling domain in the cytoplasm. Dectin-2 functions as an innate immune receptor that signals the host of an active fungal infection (45, 47–50).

We recently constructed Dectin-1-coated amphotericin B (AmB)-loaded liposomes and showed these are targeted to the  $\beta$ -glucans in the inner cell walls and bind efficiently to multiple cell types of *Aspergillus fumigatus* and to *C. neoformans* yeast cells. Dectin-1-coated AmB-loaded liposomes (DEC1-AmB-LLs) efficiently inhibit and kill

*A. fumigatus* cells (51). However, Dectin-1-coated liposomes bind poorly to *C. albicans*, presumably due to the presence of a thick mannan polysaccharide and mannoprotein outer layers masking their  $\beta$ -glucans (52–56). Herein, we coated AmB-loaded liposomes with the mannan-binding domain of mouse Dectin-2, sDectin-2. The sDectin-2-coated AmB-loaded liposomes bound efficiently to *C. albicans*, *C. neoformans*, and *A. fumigatus* and dramatically reduced cell growth and viability relative to untargeted drug-loaded liposomes.

## RESULTS

**Preparation of fungicide-loaded sDectin-2-coated fluorescent liposomes.** A model of the fungicide-loaded, sDectin-2-coated liposomes constructed herein is shown in Fig. S1 in the supplemental material. Liposome construction methods and liposome composition paralleled closely those of sDectin-1-coated liposomes described recently (51). We remotely loaded 11 mol% amphotericin B (AmB) relative to moles of liposomal lipids into the membrane of pegylated liposomes to make AmB-loaded liposomes (AmB-LLs) (51). For reference, the widely used commercial AmB-loaded untargeted liposomal product AmBisome contains 10.6 mol% AmB relative to moles of liposomal lipid (57–59) (see Table S1 in the supplemental material). We designed the murine sDectin-2 sequence to contain a small lysine tag on its amino-terminal end (see Fig. S2 in the supplemental material), expressed it in *Escherichia coli* (see Fig. S3 in the supplemental material), and conjugated the purified sDectin-2 protein via this lysine tag to NHS-PEG-DSPE (*N*-hydroxysuccinimide plus polyethylene glycol plus 1,2-distearoyl-*sn*-glycero-3-phosphoethanolamine), making DEC2-PEG-DSPE. We then incorporated DEC2-PEG-DSPE via its DSPE lipid moiety into AmB-LLs at 1 mol% protein molecules relative to moles of liposomal lipid (1,500 molecules of sDectin-2 per liposome) to make DEC2-AmB-LLs. Similarly, and as a protein-coated liposomal control, 0.33 mol% bovine serum albumin (BSA) was incorporated via a lipid carrier into AmB-LLs to make BSA-AmB-LLs. This resulted in equivalent microgram amounts of 22-kDa sDectin-2 and 66-kDa BSA proteins on the surface of these two sets of liposomes. Uncoated AmB-LLs, which closely resemble the commercial product AmBisome, also served as a liposomal control. Two moles percent DHPE (1,2-dihexadecanoyl-*sn*-glycero-3-phosphoethanolamine, triethylammonium salt)-rhodamine was also incorporated into the liposomal membrane of all three liposome preparations. Hence, all three sets of liposomes contained the same 11 mol% AmB and 2 mol% rhodamine. The composition of DEC2-AmB-LLs is compared to that of BSA-AmB-LLs, AmB-LLs, AmBisome, and AmB/micelles (a deoxycholate [DOC] micelle suspension delivering AmB) in Table S1.

**sDectin-2-coated DEC2-AmB-LLs bound more strongly to diverse fungal species than control liposomes.** sDectin-2-coated, red fluorescent, DEC2-AmB-LLs bound strongly to *C. albicans* yeast cells, pseudohyphae, and hyphae (Fig. 1). The vast majority of sDectin-2-coated liposomes bound in large clusters to the extracellular polysaccharide matrix associated with these cells. Furthermore, DEC2-AmB-LLs bound to a large subset of the extracellular matrix (Ex<sup>+</sup>) surrounding these cells, while some regions of the matrix clearly did not bind sDectin-2-coated liposomes (Ex<sup>-</sup>) (Fig. 1E). Although 100-nm liposomes are too small to be resolved by light microscopy, the presence of an estimated 3,000 rhodamine molecules per liposome (Fig. S1) allows the fluorescent signal from individual liposomes to be visualized (51). We only rarely saw individual DEC2-AmB-LLs (yellow arrows in Fig. 1A) or liposome clusters binding directly to *C. albicans* cell walls. In contrast, we previously showed individual sDectin-1-coated liposomes bound frequently to the cell wall of *A. fumigatus* cells (51).

DEC2-AmB-LLs bound strongly to *C. neoformans* yeast cells (Fig. 2). Monoclonal antibody 18B7 is specific for the glucuronoxylomannan (GXM) found in the capsule and exopolysaccharide of *C. neoformans* (60, 61). We found antibody 18B7 stained most (Fig. 2B) but not all of the cell capsules and most but not all of the exopolysaccharide that were visible in bright-field images (Ex<sup>+</sup> in Fig. 2A). DEC2-AmB-LLs contained strongly most of the 18B7-stained GXM regions in the exopolysaccharide matrix, but

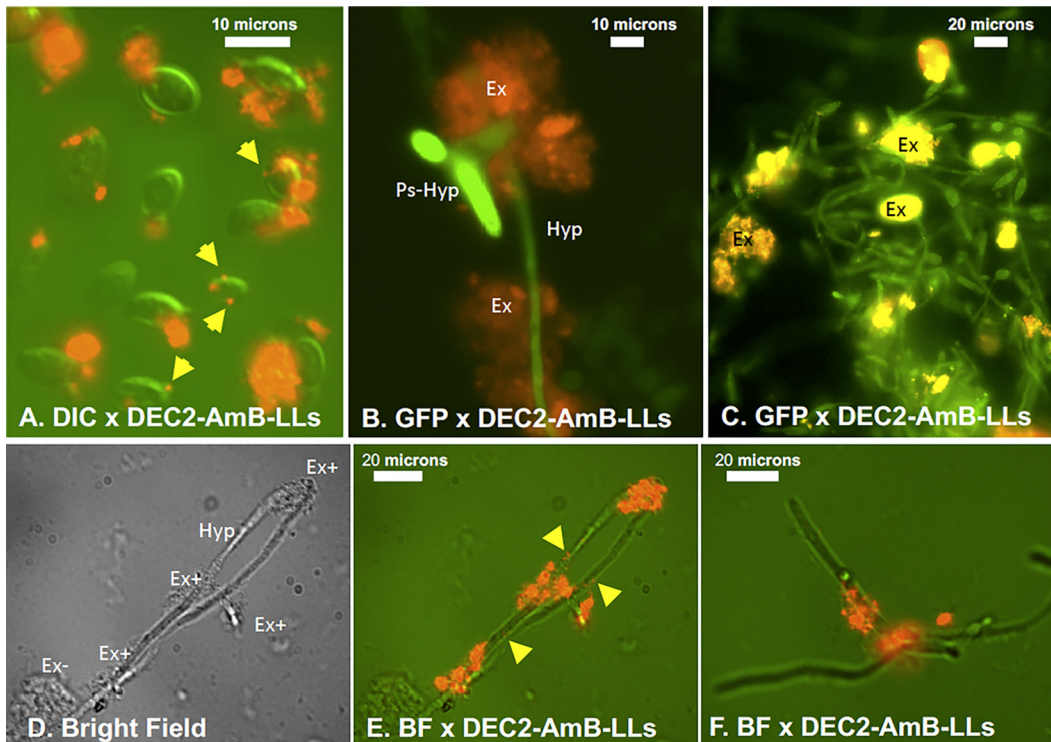


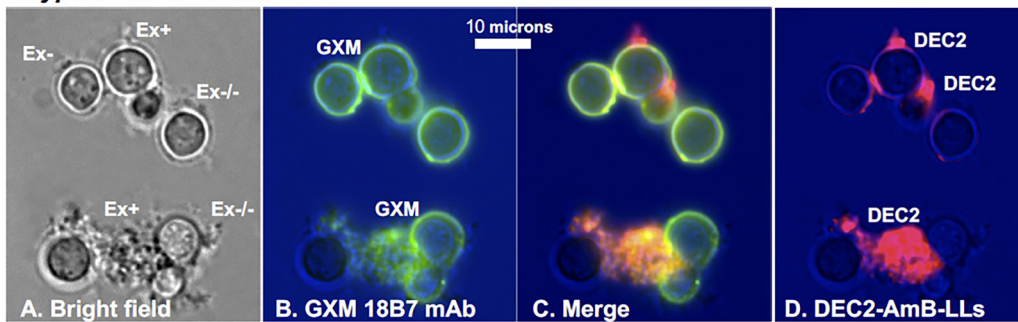
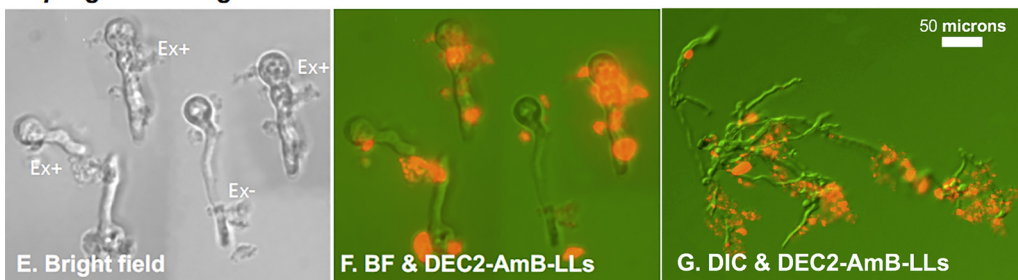
**FIG 1** sDectin-2-coated liposomes (DEC2-AmB-LLs) bound to the extracellular matrix associated with *C. albicans* cells of diverse morphologies. (A) Yeast cells. Cells are highlighted by differential interference contrast (DIC) microscopy (green), and rhodamine fluorescently labeled DEC2-AmB-LLs are in red. (B and C) Pseudohyphae (Ps-Hyp) and hyphae (Hyp). Cells are highlighted via their endogenous GFP fluorescence. DEC2-AmB-LLs bound in large clusters to the extracellular matrix (Ex). (D to F). Mature hyphae. (D) Bright-field microscopy showing extracellular matrix surrounding hyphae of stained cells in panel E. (E) Combined bright-field image and red fluorescence of liposomes. (F) Additional image parallel to that in panel E reiterating a typical staining of the matrix. All cells were stained for 1 h with a 1:200 dilution of DEC2-AmB-LLs into LDB2 buffer (e.g., 0.5  $\mu\text{g}$  sDectin-2/100  $\mu\text{l}$ ). The extracellular matrices clearly stained (Ex<sup>+</sup>) or weakly or not stained (Ex<sup>-</sup>) with DEC2-AmB-LLs are indicated. Yellow arrows indicate individual liposomes. Photographs were taken at  $\times 63$  magnification under oil immersion. Several independent fungal cell labeling studies gave similar images.

did not stain the 187B-labeled GXM of the capsule (Fig. 2C and D). Furthermore, there were some regions of extracellular matrix that did not stain with either 18B7 or DEC2-AmB-LLs (Ex<sup>-</sup> in Fig. 2A).

DEC2-AmB-LLs also bound in large clusters to the exopolysaccharide matrices produced by *A. fumigatus* germinated conidia and hyphae (Fig. 2E to G). Again, little if any binding was associated with the cell wall itself. Also, there appear to be areas where the exopolysaccharide matrix is not stained or poorly stained (Ex<sup>-</sup> in Fig. 2E and F).

Because the DEC2-AmB-LLs bound poorly or not at all to mannans within the tightly cross-linked polysaccharide of cells walls of all three fungal species examined, we considered that the 100-nm-diameter size of our liposomes restricted their access or that sDectin-2 was somehow restricted from full activity when presented in a liposomal membrane. The rotational diameter of DEC2-AmB-LLs in solution would be even larger than their physical size estimate, due to their coating with sDectin-2 protein and associated water molecules. sDectin-2 itself has an atomic weight of 22 kDa and hence a rotational diameter in solution that may be estimated at  $\sim 4$  nm (62). We prepared rhodamine-coupled sDectin-2, DEC2-Rhod. The atomic weight of rhodamine (0.48 kDa) and one or two rhodamine-coupled molecules will have little effect on this size estimate for DEC2-Rhod. Red fluorescent DEC2-Rhod bound strongly to most of the exopolysaccharide matrix surrounding *A. fumigatus* hyphal cells (see Fig. S4A and B in the supplemental material). The pattern of binding and intensity of binding was indistinguishable from that of DEC2-AmB-LLs (Fig. S4C and D).

We quantified the efficiency of DEC2-AmB-LLs binding to fungal cells compared to control uncoated AmB-LLs and BSA-coated liposomes (BSA-AmB-LLs). The area of

***Cryptococcus neoformans******Aspergillus fumigatus***

**FIG 2** DEC2-AmB-LLs bound to the extracellular matrices associated with *C. neoformans* and *A. fumigatus* cells. Rhodamine red fluorescent DEC2-AmB-LLs bound in large clusters to the extracellular matrices (Ex) and rarely to the cell walls of both species. (A to D) *C. neoformans*. Yeast cells were costained with DEC2-AmB-LLs and mouse monoclonal antibody 18B7 to capsular glucuronoxylomannan (GXM) and secondary goat anti-mouse antibody Alexa 488 (green). All cells were stained for 1 h with a 1:200 dilution of DEC2-AmB-LLs into LDB2 (e.g., 0.5  $\mu\text{g}$  sDectin-2/100  $\mu\text{l}$ ). (A) Bright-field image of cells. (B) Green fluorescent image of GXM-specific antibody-stained cells. (C) The merged fluorescent image of panels B and D. (D) Red fluorescent DEC2-AmB-LLs. (E to G) *A. fumigatus*. (E and F) Bright-field and combined fluorescent images of germlings grown for 10 h and stained with DEC2-AmB-LL. (G) Mature hyphae grown for 24 h. Both species were stained for 1 h with a 1:200 dilution of DEC2-AmB-LLs into LDB2 (e.g., 0.5  $\mu\text{g}$  sDectin-2/100  $\mu\text{l}$ ). The extracellular matrices clearly stained (Ex<sup>+</sup>) or weakly or not stained (Ex<sup>-</sup>) with DEC2-AmB-LLs or which did not stain with either 18B7 or DEC2-AmB-LLs (Ex<sup>-/-</sup>) are indicated. Photographs were taken at a  $\times 63$  magnification under oil immersion (A to F) or at  $20\times$  (G). Three independent fungal cell labeling studies gave similar images.

fluorescent liposome signal was measured from multiple red fluorescent photographic images taken of liposome-stained cultures that were nearly confluent with fungal cells (Fig. 3). DEC2-AmB-LLs bound to *C. albicans* pseudohyphae and hyphae, *C. neoformans* yeast cells, and *A. fumigatus* hyphae 50- to 150-fold more efficiently than AmB-LLs or BSA-AmB-LLs (Fig. 3A, D, and G). Examples of the photographic images of fluorescent liposomes quantified to make these measurements are presented adjacent to each bar graph (Fig. 3B, C, E, F, H, and I).

Using the same quantitative assay of the area of fluorescent liposome binding to *C. albicans* pseudohyphae and hyphae, we characterized the specificity, stability, and rate of DEC2-AmB-LL binding (Fig. 4). DEC2-AmB-LL labeling was 75% inhibited by the inclusion of solubilized yeast mannans during the binding assay, but not by the same concentrations of the soluble  $\beta$ -glucan laminarin or of the glucose-fructose-containing disaccharide sucrose (Fig. 4A to C). This result confirmed that sDectin-2-targeted liposome binding to the extracellular matrix was mannan specific, in agreement with the published carbohydrate specificity of sDectin-2 (42–46). We examined the stability of binding of DEC2-AmB-LLs to *C. albicans* cells by taking the DEC2-AmB-LL-stained preparations examined in Fig. 3A and storing them in the dark in phosphate-buffered saline (PBS) at 4°C. After 2 months, these cells were rephotographed and liposomal staining quantified. The fluorescent intensity of DEC2-AmB-LLs bound to cells remained strong and was estimated to be 50-fold stronger than the nonspecific binding of AmB-LLs (Fig. 4D to F). This result suggests that the DEC2-AmB-LLs themselves are relatively stable and that their binding to cells is also relatively stable. The rate of DEC2-AmB-LL binding was estimated by exposing dense fields of *C. albicans* pseudo-

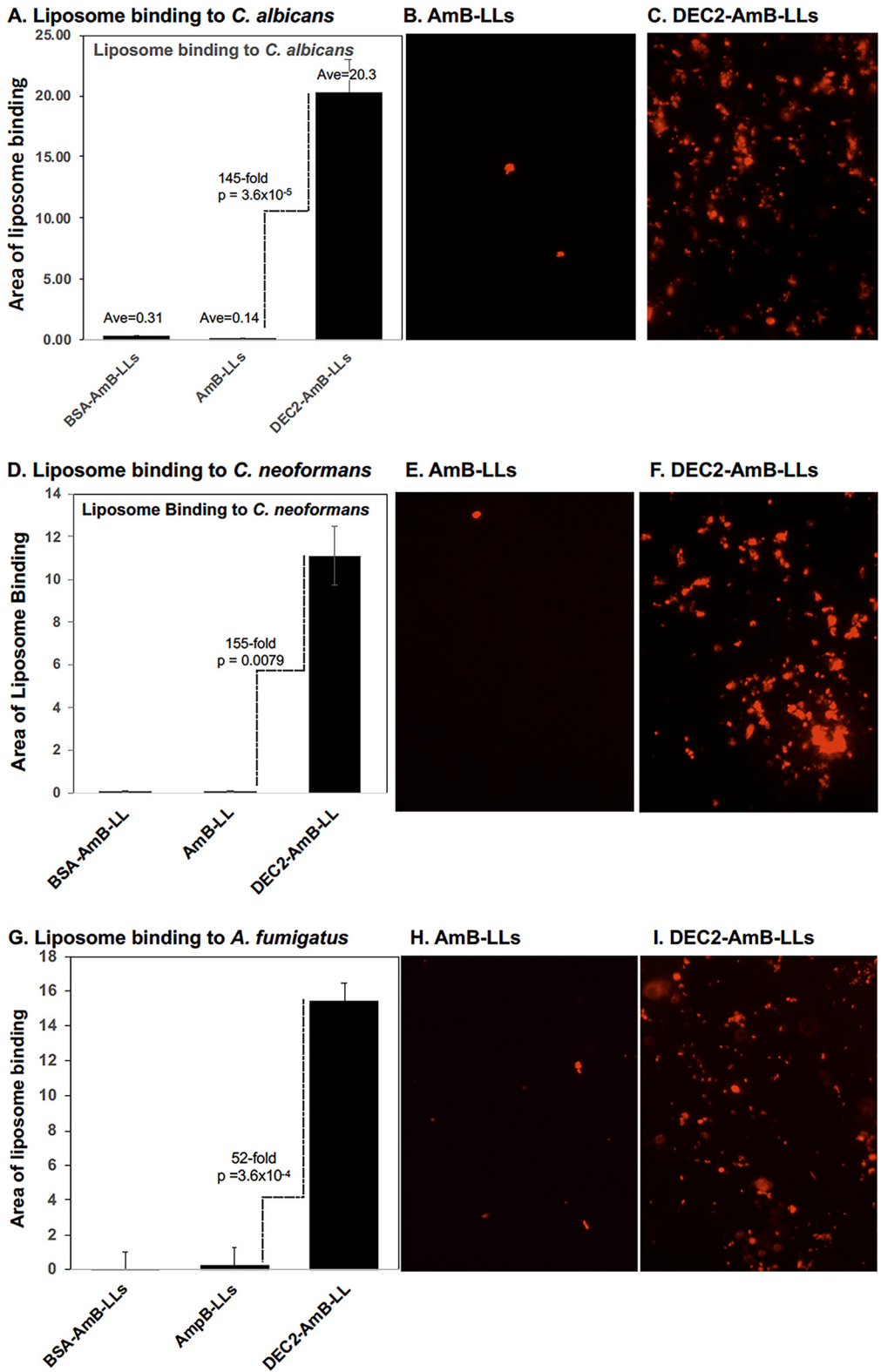


**FIG 3** sDectin-2-coated DEC2-AmB-LLs bound 1 to 2 orders of magnitude more efficiently to *C. albicans*, *C. neoformans*, and *A. fumigatus* cells than control AmB-LLs. Dense fields of fixed fungal cells were incubated for 1 h with 1:200 dilutions of liposomes in liposome dilution buffer LDB2 (e.g., 0.5  $\mu\text{g}$  sDectin-2/100  $\mu\text{l}$ ). Unbound liposomes were washed out after 1 h. Multiple fields of red fluorescent images were photographed at 20 $\times$ , and the area of red fluorescence was estimated in Image J. Examples of photographic images are shown to the right of the bar graphs. (A to C) *C. albicans*. (D to F) *C. neoformans*. (G to I) *A. fumigatus*. In panels A, D, and G, standard errors from the mean are presented and fold differences and *P* values are indicated to distinguish the binding of DEC2-AmB-LLs from AmB-LLs.

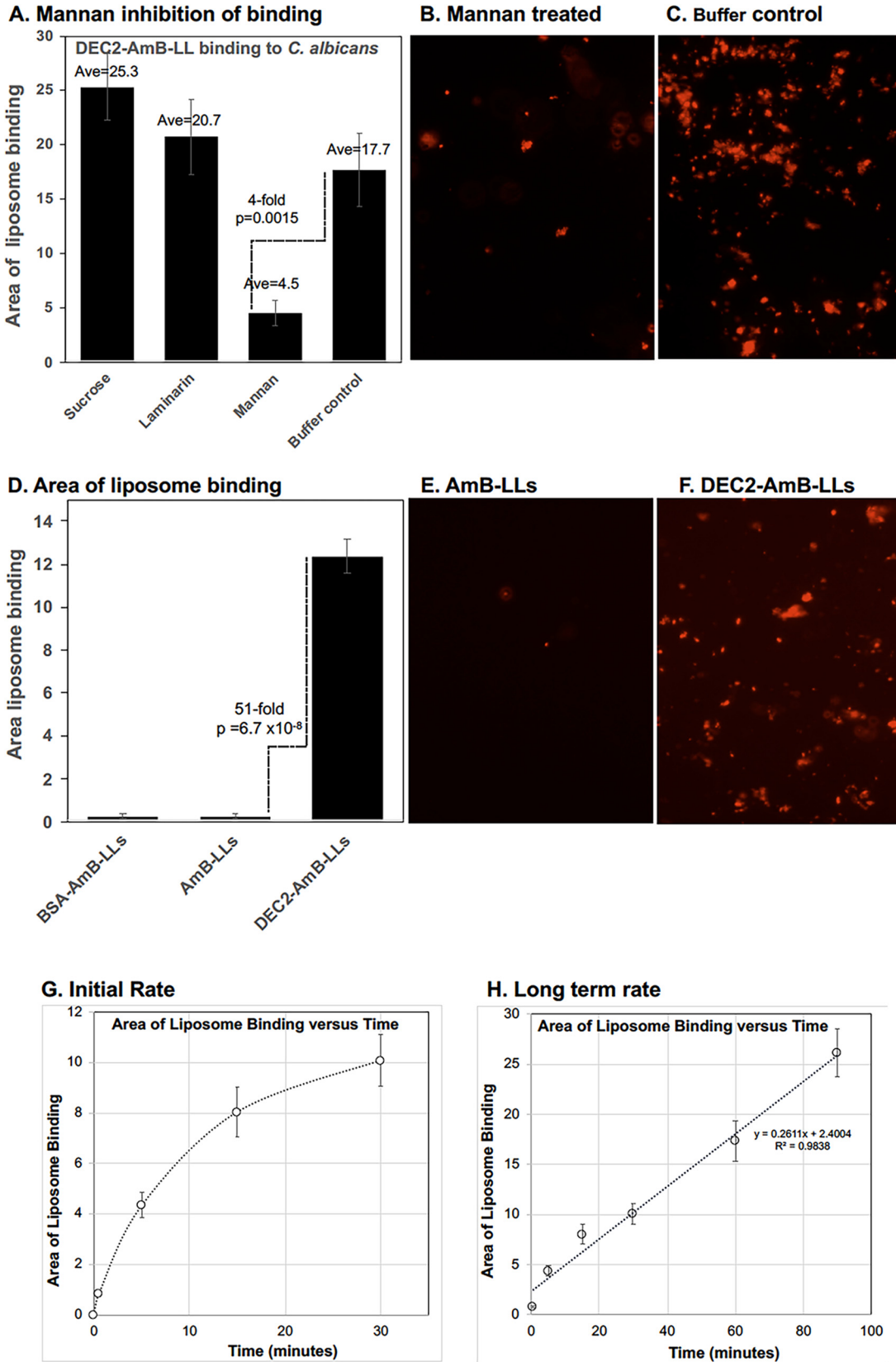


**FIG 4** Specificity, stability, and rate of DEC2-AmB-LL binding. (A to C) Specificity of binding. DEC-AmB-LL labeling of *C. albicans* was inhibited by soluble yeast mannan, but not by sucrose or laminarin. Each polysaccharide was added at 10 mg/ml during a 1-h staining procedure. (D to F) Stability of binding. The plates of *C. albicans* cells stained with DEC2-AmB-LLs and control liposomes used to generate the data in Fig. 3A to C were left in PBS, stored in the dark for 2 months, and rephotographed, and the area of

(Continued on next page)

hyphal and hyphal cells to liposomes for periods ranging from 10 s to 90 min before washing off unbound liposomes (Fig. 4G and H). The area of DEC2-AmB-LL labeling increased rapidly and exponentially for the first 15 min (Fig. 4G) and then slowed, but labeling did not appear to be complete after 90 min (Fig. 4H).

In summary, Dectin-2-coated AmB-loaded liposomes (DEC2-AmB-LLs) bound specifically, stably, and rapidly to fungal mannans present in the extracellular matrix of *C. albicans* grown *in vitro*, while little nonspecific binding of control liposomes was observed. There were only trace amounts of DEC2-AmB-LL binding to the cell wall. DEC2-AmB-LLs also bound efficiently to portions of the extracellular matrices surrounding *C. neoformans* and *A. fumigatus* cells.

**Growth inhibition and killing by DEC2-AmB-LLs.** We performed various fungal cell growth and viability assays after treating actively growing cultures of *C. albicans*, *C. neoformans*, and *A. fumigatus* with sDectin-2-coated and control liposomes delivering AmB concentrations near the MICs for this fungicide (Fig. 5). Depending upon the assay conditions and delivery method for AmB, the MICs for AmB estimated for these species range from 0.06 to 1.3  $\mu\text{M}$  (63–67). It seemed reasonable to consider that at reported AmB concentrations near the MICs for these species, we might best resolve the improved performance of targeted AmB-loaded liposomes relative to untargeted drug.

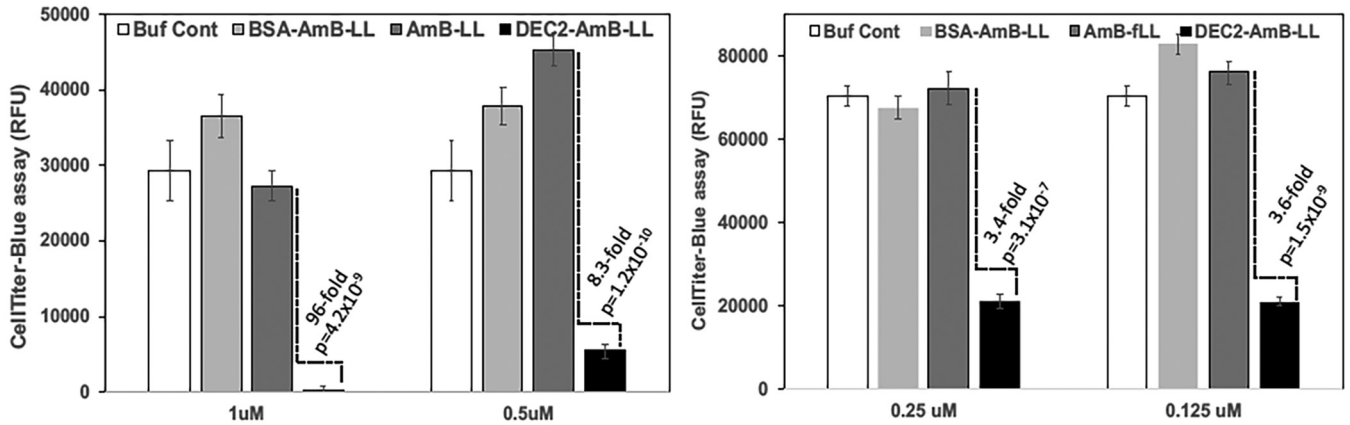
We inoculated 4,000 *C. albicans* yeast cells into individual wells of 96-well microtiter plates, grew them for 6 h to the pseudohyphal and early hyphal stages, and treated the cells with drug-loaded liposomes. After a 30-min incubation, liposomes were washed out and cells were grown for an additional 16 h. Figure 5A shows that targeted DEC2-AmB-LLs delivering from 1  $\mu\text{M}$  down to 0.125  $\mu\text{M}$  AmB killed or inhibited of *C. albicans* cells from 90-fold to 3-fold more efficiently than uncoated AmB-LLs or BSA-AmB-LLs delivering the same concentrations of AmB. The difference is remarkable given that in these experiments, cells were exposed to liposomal drug for only 30 min. These data were obtained using CellTiter-Blue (CTB) reagent to assess cytoplasmic reductase activity as a proxy for cell integrity and viability. Dead cells or metabolically inactive cells do not reduce the resazurin substrate to fluorescent resorufin product. Treatment of *C. albicans* cells continuously with liposomes for the entire 16-h time period or with higher drug concentrations resulted in too much cell death for all three drug-loaded liposome samples to clearly resolve differences among the different liposome preparations. Six-month-old preparations of DEC2-AmB-LLs retained their full antifungal activity, as long as they were freshly reduced (Materials and Methods). We also assayed viable cell numbers after liposome treatment. *C. albicans* yeast cells growing in rich medium in liquid culture were incubated with liposomes delivering 2  $\mu\text{M}$  AmB. The liposomes were washed out after 30 min. After an additional 6 h of growth, the cultures were diluted and assayed for CFU on agar plates with rich medium. Based on CFU, DEC2-AmB-LLs were 3-fold more effective at inhibiting or killing *C. albicans* yeast cells in liquid than AmB-LLs or BSA-AmB-LLs (Fig. S2A).

*C. neoformans* yeast cells growing in liquid were treated for 4 h with liposomes delivering 0.4  $\mu\text{M}$  AmB and overnight with liposomes delivering 0.4, 0.2, and 0.1  $\mu\text{M}$  AmB (Fig. 5B). At the end of each treatment, cells were diluted and CFU were assayed on agar plates with rich medium. DEC2-AmB-LLs were 2.5- to 11-fold more effective at killing *C. neoformans* than AmB-LLs or BSA-AmB-LLs, with the optimum treatment being 0.2  $\mu\text{M}$  AmB overnight. As an alternative assay, *C. neoformans* yeast cells growing on

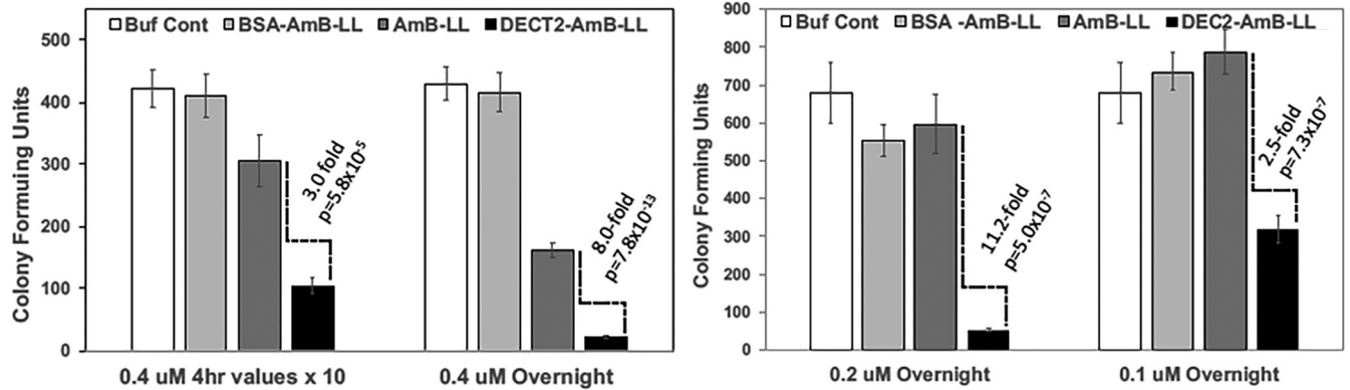
#### FIG 4 Legend (Continued)

liposome binding was quantified. (G and H) Rate of binding. Mature cultures of *C. albicans* composed of some pseudohyphae and hyphae were grown on the surface of a 24-well microtiter plate in VMM plus 20% FBS, fixed, blocked, and treated with DEC2-AmB-LLs for the indicated times. In all three experiments, DEC2-AmB-LLs were diluted in 1:200 (wt/vol) LDB2 (0.5  $\mu\text{g}$  in 100  $\mu\text{l}$  sDectin-2) and washed 4 times with LDB2. Multiple red fluorescent images were taken at  $\times 20$  magnification for each time point on an inverted fluorescence microscope, and the average area of red fluorescent liposome staining was estimated. Standard errors from the mean are shown in panels A, D, G, and H. In panels A and D, the numerical average and number of fields examined are indicated above each bar and on the vertical axis. In panels A and D, fold differences and *P* values are indicated for the performance of DEC-AmB-LLs relative to mannan inhibition (A) or relative to AmB-LLs (D). These results are representative of two biological replicates.

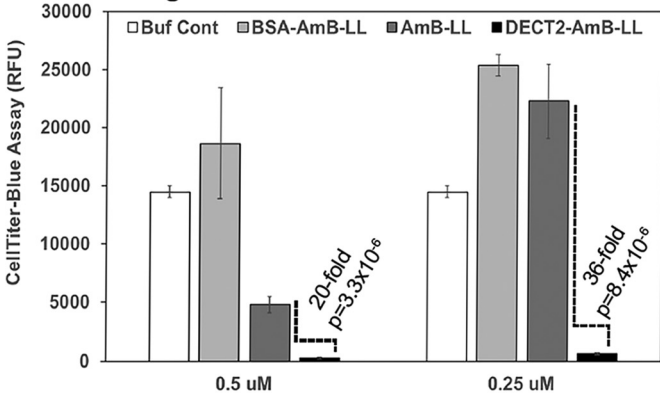
### A. Inhibition and killing of *C. albicans*.



### B. Inhibition and killing of *C. neoformans*



### C. *A. fumigatus* with DEC2-AmB-LLs



### D. *A. fumigatus* with DEC1-AmB-LLs

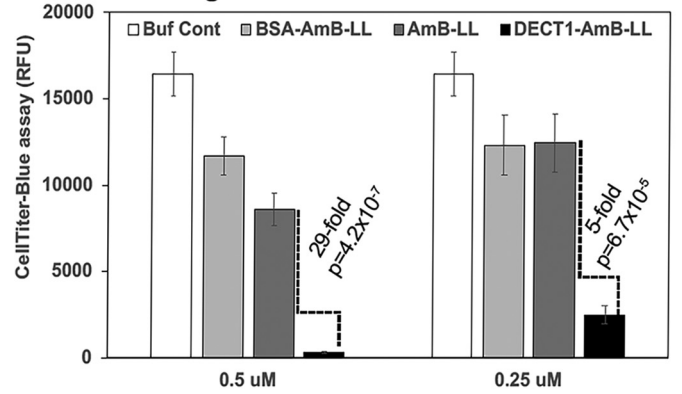


**FIG 5** sDectin-2-coated amphotericin B-loaded liposome inhibition and killing of *C. albicans*, *C. neoformans*, and *A. fumigatus*. (A) *C. albicans* with DEC2-AmB-LLs. Cells in the pseudohyphal and early hyphal stage grown in RPMI medium plus 0.5% BSA on 96-well polystyrene microtiter plates. Cells were treated for 30 min with liposomes delivering 1.0., 0.5, 0.25, and 0.12  $\mu$ M AmB to the medium as indicated, washed twice with medium, grown for an additional 16 h, and then assayed for metabolic activity using CellTiter-Blue (CTB) reagent. (B) *C. neoformans* with DEC2-AmB-LLs. *C. neoformans* cells were grown in liquid YPD medium plus 0.5% BSA with vigorous shaking for 2 h and treated for 4 h or overnight with liposomes delivering 0.4, 0.2, or 0.1  $\mu$ M AmB to the medium as indicated. Cells were diluted and plated on YPD medium, and CFU were counted from multiple plates. (C) *A. fumigatus* with DEC2-AmB-LLs. Conidia were germinated for 9 h in VMM plus glucose plus 0.5% BSA in 96-well polystyrene microtiter plates, treated for 2 h with liposomes delivering 0.5 and 0.25  $\mu$ M AmB to the medium as indicated, washed twice with medium, grown overnight, and then assayed for metabolic activity using CTB reagent in RPMI lacking phenol red indicator plus 0.5% BSA. The control wells were overgrown with hyphae protruding out the medium. (D) *A. fumigatus* with DEC1-AmB-LLs. Assay conditions were similar to the assay in panel C, except liposomes were first diluted into LDB1 buffer (PBS plus 0.5% BSA plus 1 mM BME) prior to dilution into growth medium. For CTB assays in panels A, C, and D, the fluorescence background from medium incubated with CTB reagent was subtracted. Standard errors are shown for all values, and fold differences and *P* values were estimated comparing the performance of AmB-LLs to DEC2-AmB-LLs. Two or more biological replicates gave similar results.

microtiter plates were treated for 5 h with liposomes delivering 1  $\mu\text{M}$  AmB. Cells were immediately assayed for cell death by incubating them with propidium iodide. Propidium iodide enters dead but not live cells and fluoresces red when it intercalates into double-stranded DNA or short regions of double-stranded RNA. Propidium iodide assays showed that under these treatment conditions, DEC2-AmB-LLs were 5-fold more efficient at killing *C. neoformans* cells than uncoated AmB-LLs (Fig. S2B, C, and D).

*A. fumigatus* was treated with liposomes delivering AmB concentrations near and below the MIC estimated for AmBisome: 0.5  $\mu\text{M}$  (67). Conidia were germinated and grown until the very early germling stage, when the germ tube first began to emerge from 95% of conidia. Cells were then treated for 2 h with AmB-containing liposomes or liposomal dilution buffer, and unbound liposomes were washed off with growth medium. Cells were grown for an additional 19 h and assayed for viability and metabolic activity with CellTiter-Blue reagent. DEC2-AmB-LLs delivering 0.5 and 0.25  $\mu\text{M}$  AmB killed or inhibited the growth of *A. fumigatus* 20-fold and 36-fold more efficiently than AmB-LLs, respectively (Fig. 5C). It should be noted that the dilution buffer control-treated *A. fumigatus* cells overgrow and generate a thick hyphal mat in the microtiter wells during this assay. Hence, the metabolic activity and CellTiter Blue signal from these control cells was low.

Dectin-1-targeted AmB-loaded liposomes also bind efficiently to *A. fumigatus* swollen conidia, germlings, and hyphal cells and inhibit and kill these cells (51), although they are binding  $\beta$ -glucans and not  $\alpha$ -mannans. In this previous study, cells were incubated continuously with liposomes during the entire assay and not washed out. For a more direct comparison of the drug-targeting efficiency of the two Dectins, we examined DEC1-AmB-LLs using the same assay design used herein for DEC2-AmB-LLs, washing out the liposomes after 2 h, except that liposomes were initially diluted into LDB1 and the cells were grown out for 16 h (see Materials and Methods). DEC1-AmB-LLs delivering 0.5 and 0.25  $\mu\text{M}$  AmB killed or inhibited the growth of *A. fumigatus* 28-fold and 5-fold more efficiently than AmB-LLs, respectively (Fig. 5D). Using this assay condition, the results from AmB-loaded liposomes targeted by Dectin-1 and Dectin-2 are very similar.

**Toxicity of DEC2-AmB-LLs to animal cells.** Rapidly grown cultures of human HEK-293 and human HT-29 cells were treated overnight with various liposomes and a deoxycholate micelle suspension each delivering 15  $\mu\text{M}$  AmB (AmB/micelles). Based on CellTiter-Blue assay of metabolic activity and viability, DEC2-AmB-LLs were 10% to 20% more toxic than AmB-LLs or BSA-AmB-LLs and 2- to 5-fold less toxic than AmB deoxycholate (AmB/DOC) micelles (Fig. S3). When these cells were treated to receive lower AmB concentrations (for example, 3  $\mu\text{M}$  AmB), only AmB/DOC micelles showed measurable toxicity. None of the three liposomal preparations appeared to have any particular affinity for either of these cell lines when examined by fluorescence microscopy.

## DISCUSSION

We coupled the N-terminal domain of Dectin-2, sDectin-2, to a lipid carrier and inserted this conjugate into liposomes such that the C-terminal carbohydrate recognition domain (CRD) of each monomer faced outward from the liposomal membrane. Considering the efficient binding we observed for these DEC2-AmB-LLs to the extracellular matrices of three diverse human fungal pathogens, the sDectin-2 monomers must have been conformationally free to form the functional dimers necessary for efficient mannan binding (48, 68). C-type lectin receptors often bind some of their substrates weakly. The published estimated effective concentrations for 50% of sDectin-2 binding to mannan-related polysaccharides ( $\text{EC}_{50}$ s) range from approximately 20 mM for mannose and 2 mM for mannan- $\alpha$ -1-2-mannan (68) down to 150  $\mu\text{M}$  for mannoglycan (44, 68). This is indeed weak binding compared to Dectin-2's closest paralog, Dectin-1, which has  $\text{EC}_{50}$ s for binding various  $\beta$ -glucans ranging from 2 mM down to 2.2 pM (69). It is likely that the greater avidity created by having approximately 1,500 sDectin-2

monomers on each liposome resulted in the rapid, strong, and stable binding we observed for DEC2-AmB-LL binding to fungal cells.

Most pathogenic fungal species, including *Candida*, *Cryptococcus*, and *Aspergillus*, live within polysaccharide matrices that promote adherence to host cells, tissues, and implanted biomedical devices, and which partially protect them from host antifungal activities (70–73). The exopolysaccharide matrix of *C. albicans* contains approximately 13%  $\beta$ -1,6-glucan and 87%  $\alpha$ -1,6-mannan (74). *C. neoformans* produces a glucuronoxylomannan- and galactoxylomannan-rich capsule (75) that is shed and contributes to formation of the extracellular matrix. The matrix is composed of 20% mannan and 23% glucan residues (76). The exopolysaccharide matrix of *A. fumigatus* contains approximately 14% galactomannan and 13%  $\beta$ -glucans (77). Our data on the efficient binding of DEC2-AmB-LLs to the extracellular matrix of all three species is consistent with the mannan-rich content of their exopolysaccharides. However, some regions of the *C. albicans*, *C. neoformans*, and *A. fumigatus* matrices did not stain or stained poorly with sDectin-2-coated liposomes, suggesting that either the distribution of mannans in the matrix is heterogeneous or the mannans in these regions are masked from exposure to liposomal sDectin-2. This distinction between mannan exposure or expression within their exopolysaccharide matrices remains to be resolved. We showed that the binding of DEC2-AmB-LLs to exopolysaccharide mannans was no more restricted than the binding of the much smaller DEC2-Rhod, suggesting size restriction may not be the primary limitation.

We did not find convincing evidence that DEC2-AmB-LLs bound more than at trace levels to the cell walls of any of these fungal species. Although the cell wall mannan content varies widely based on growth media and methods of chemical analysis, the estimated cell wall mannan polysaccharide content of *C. neoformans* is 22% (78), that of *C. albicans* is 40% (79), and that of *A. fumigatus* is 15% to 41% (73, 79). Although rhodamine-labeled sDectin-2 (DEC2-Rhod) bound with similar intensity and pattern to the exopolysaccharide matrix of *A. fumigatus* as DEC2-AmB-LLs, DEC2-Rhod did not stain the cell wall. Hence, again a size barrier for the much larger DEC2-AmB-LLs does not appear to explain their lack of cell wall binding. Hence, our findings suggest the cell wall mannans may be chemically masked from sDectin-2-mediated liposomal binding. This result parallels the masking of *C. albicans* cell wall  $\beta$ -glucans from sDectin-1 binding and from DEC1-AmB-LL binding (52, 54–56).

*C. albicans* reversibly switches among unicellular ovoid yeast and multicellular ellipsoid pseudohyphal and elongated hyphal morphologies (80). All three stages are capable of producing an extracellular matrix and adhering to host tissues. The matrices of all three bound DEC2-AmB-LLs, suggesting fungicide-loaded Dectin-2-coated liposomal therapeutics have the potential to reduce the virulence of *C. albicans*.

DEC2-AmB-LLs inhibited and killed *C. albicans*, *C. neoformans*, and *A. fumigatus* far more efficiently than plain uncoated AmB-LLs or BSA-AmB-LLs delivering the same concentrations of AmB. A combination of metabolic activity assays based on CellTiter-Blue (CTB) reagent, cell growth assays based on CFU, and propidium iodide staining of dead cells confirmed that both inhibition and killing of cells occurred. Incubation with DEC2-AmB-LLs for as little as 30 min to a few hours resulted in significant killing. DEC2-AmB-LLs were 3- to 90-fold more efficient at inhibiting or killing fungal cells, when delivering AmB concentrations near or below the MIC values reported for AmB, concentrations at which our AmBisome equivalent uncoated AmB-LLs had little or no impact on cell inhibition or survival. The DEC2-AmB-LLs bound all three species 50- to 150-fold better than AmB-LLs and, under some conditions we tested, inhibited and killed them 11- to 94-fold more efficiently than AmB-LLs. We believe the differences in the optimal results for the binding and killing assays and the variability within the killing assays are due primarily to the fact that inhibition and killing assays are much more complex and difficult to optimize. They are influenced by many variables, including (i) the amount of AmB being delivered, (ii) the cells proceeding through more than one developmental stage during the assay, (iii) the time of liposome exposure, (iv) the length of the growth period after liposome exposure, and (v) the mechanics of the

assay being used. The binding assays are influenced primarily by the concentration of sDectin-2 and the extent of washing.

A significant reduction in the MIC for AmB or other liposomal packaged therapeutic fungicides should result in reducing fungicide doses and the frequency of drug administration, which, in turn, should reduce host toxicity. We showed that DEC2-AmB-LLs were not particularly toxic to animal cells when delivering 15  $\mu$ M AmB, which was 15- to 150-fold higher than the AmB concentrations used here to kill fungal cells. However, there are number of important factors that we have not yet explored *in vitro*, which may alter the amount of exopolysaccharide matrix and its composition and may influence the effectiveness of Dectin-2-targeted antifungals *in vivo*. These include growth substrate, temperature, carbon source, serum, and the particular antifungals being delivered.

*Candida*, *Cryptococcus*, and *Aspergillus* species belong to three evolutionarily disparate classes of fungi (81), the Saccharomycetes (phylum Ascomycota), Tremellomycetes (phylum Basidiomycota), and Eurotiomycetes (phylum Ascomycota), respectively. It is estimated that they separated from common ancestry relatively early in the evolution of the fungal kingdom, 0.8 to 1.3 billion years ago (82). DEC2-AmB-LLs bound specifically to the extracellular matrix of all three. This suggests the mannans found in the extracellular matrices of most pathogenic fungi will be conserved enough in structure to bind sDectin-2-targeted liposomes. However, mannan expression and masking from host detection may vary widely among pathogenic fungal species or in different host niches. Consistent with the masking of mannans to sDectin-2 binding, our assays showed very inefficient binding to the mannan-rich cell walls of all three species.

This preliminary study was performed with the mouse sDectin-2 protein sequence to avoid problems of sDectin-2 immunogenicity during the future testing of sDectin-2-targeted antifungals in mouse models of candidiasis, aspergillosis, and cryptococcosis. The human sDectin-2 protein sequence is 72% identical to the mouse protein and is only 2 amino acids (aa) shorter. Therefore, we do not expect problems manipulating the human protein to target fungicide-loaded therapeutic liposomes for use in clinical studies.

In summary, there is a dire need for new antifungal therapeutics. DEC2-AmB-LLs bound efficiently to the extracellular matrices produced by diverse cellular stages of *C. albicans*, *C. neoformans*, and *A. fumigatus*. DEC2-AmB-LLs delivering AmB concentrations near or below AmB's MICs for growth inhibition and killing of all three species showed sDectin-2 targeting of the liposome-packaged drug improved the fungicidal effect by an order of magnitude or more over untargeted liposomal AmB. It is reasonable to propose that, drug-loaded liposomes targeted to fungal cells have significant potential as pan-antifungal therapeutics with a wide range of applications. The next step in our research will be to examine the efficacy of targeted liposomal antifungal drugs in mouse models of invasive fungal diseases.

## MATERIALS AND METHODS

**Cell culture.** *C. albicans* CAI4 expressing green fluorescent protein (GFP) under the control of the *ADH1* promoter (83), *A. fumigatus* A1163 (51), and wild-type *C. neoformans* H99-alpha (84) were grown in Vogel's minimal medium (VMM) plus 1% glucose (85) plus 0.5% BSA or RPMI 1640 medium with no red indicator dye (Thermo Fisher SKU-11835-030) plus 0.5% BSA or YPD (1% yeast extract, 2% peptone, 2% dextrose) in liquid with shaking or on 24- or 96-well polystyrene microtiter plates or on glass microscope chamber slides and incubated at 37°C for 3 to 36 h. Plates were precoated with poly-L-lysine for *A. fumigatus*, and glass microscope slides were precoated with for all three species. All fungal cell growth was carried out in a biosafety level 2 (BSL2) laboratory. Before cells were treated with fluorescent liposomes for microscopic analysis of binding, fungal cells were washed three times with PBS, fixed in 4% formaldehyde in PBS for 60 min, washed three times, and stored at 4°C in PBS.

The human colorectal adenocarcinoma cell line HT-29 (ATCC HTB-38) and human embryonic kidney cell line HEK-293 (ATCC CRL-1573) were grown in 96-well microtiter plates in RPMI medium lacking red indicator dye plus 10% fetal calf serum in a 37°C incubator in air supplemented with 5% CO<sub>2</sub>. Their viability and metabolic activity after overnight antifungal treatment were assayed using CTB reagent diluted 1:10 into the medium and with incubation for 60 to 90 min at 37°C with 8 wells per treatment.

**Production and chemical modification of sDectin-2.** The carboxy-terminal end of Dectin-2 contains its mannan recognition domain, sDectin-2. The sequence of the codon-optimized *E. coli* expression construct with MmsDectin-2lyshis synthesized and cloned into pET-45B by GenScript is shown in Fig. S2.

The 577-bp-long DNA sequence encodes a slightly modified 189-amino-acid (aa)-long sDectin-2 protein containing a vector-specified N-terminal (His<sub>6</sub>) affinity tag, an additional flexible GlySer spacer, the sequence LysGlyLys with lysine residues for cross-linking, another flexible spacer followed by the C-terminal 166-aa-long murine sDectin-2 domain. The modified sDectin-2 protein, DEC2 was expressed in *E. coli* and purified as described previously for mouse sDectin-1 (51) followed by an extra step of gel exclusion chromatography on Sephacryl S-100 HR (GE Healthcare, no. 17061210). The protein is shown on an SDS-PAGE gel stained with Coomassie blue in Fig. S3. Samples of sDectin-2 at 5  $\mu\text{g}/\mu\text{l}$  in the same guanidine hydrochloride (GuHCl) buffer with freshly added 5 mM  $\beta$ -mercaptoethanol (BME) were adjusted to pH 8.3 with 1 M pH 10 triethanolamine and reacted with the reactive succinimidyl ester NHS moiety of a 4 M excess of DSPE-PEG-3400-NHS (1,2-distearoyl-*sn*-glycero-3-phosphoethanolamine [DSPE]-conjugated polyethylene glycol [PEG], from Nanosoft Polymers; no. 1544-3400) for 1 h at 23°C to make DEC2-PEG-DSPE (Fig. S1). Size exclusion chromatography through Bio-Gel P-6 acrylamide resin (Bio-Rad no. 150-0740) in renaturation and storage buffer RN#5 (0.1 M NaH<sub>2</sub>PO<sub>4</sub>, 10 mM triethanolamine, pH 8.0, 1 M L-arginine, 100 mM NaCl, 5 mM EDTA, 5 mM  $\beta$ -mercaptoethanol) removed unincorporated DSPE-PEG and GuHCl (51). BSA-PEG-DSPE was prepared from BSA (bovine serum albumin; Sigma, A-8022) by the same protocol, but with buffer lacking the GuHCl during DSPE-PEG labeling and L-arginine during Bio-Gel P6 chromatography. Rhodamine-labeled sDectin-2 (DEC2-Rhod) was prepared by the same procedure used to make DEC2-PEG-DSPE in the same GuHCl buffer, but labeling was performed with a 4 M excess of rhodamine-NHS reagent (Thermo Fisher no. 46406) over sDectin-2. Hydrolyzed unbound rhodamine reagent and unwanted salts were removed from DEC2-Rhod using size exclusion chromatography on Bio-Gel P2 resin in RN#5 buffer.

**Remote loading of AmB, sDectin-1, BSA, and rhodamine into liposomes.** Starting with sterile pegylated liposomes from FormuMax Scientific, Inc. (DSPC:CHOL:mPEG2000-DSPE; FormuMax no. F10203A), we prepared small batches of liposomes with 11 mol% AmB (Sigma A4888) relative to 100% liposomal lipid to make AmB-LLs as described previously (51) (Table S1).

The DEC2-PEG-DSPE and BSA-PEG-DSPE conjugates in RN#5 buffer and PBS, respectively, were integrated via their lipid DSPE moiety into the phospholipid bilayer membrane of AmB-LLs by 30 min of incubation at 60°C to make DEC2-AmB-LLs and BSA-AmB-LLs, parallel to the protocol used previously (51). During these same 60°C incubations, 2 mol% of the red fluorescent tag Lissamine rhodamine B-DHPE (Invitrogen, no. L1392) was also incorporated into sDectin-2- and BSA-coated liposomes and AmB-LLs (51). A duplicate sample of the DEC2-AmB-LLs was subjected to gel exclusion chromatography over 0.5 M Bio-Gel A resin (Bio-Rad, no. 151-0140). Fluorescent liposomes were efficiently excluded from the resin. Because no sDectin-2 (optical density at 280 nm [OD<sub>280</sub>] of 2.2/mg/ml) or rhodamine was detected in the low-molecular-weight fractions included in the gel, we concluded that both were efficiently loaded into liposomes. Fresh 2 mM BME was added to DEC2-AmB-LLs before each use in binding or killing assays. DEC2-AmB-LLs stored at 4°C in RN#5 appeared to retain full fungal cell binding specificity and killing activity for at least 12 months.

**Microscopy of liposomes and DEC2-Rhod bound to fungal cells.** Formalin-fixed fungal cells were incubated with liposomes at 23°C in liposome dilution buffer LDB2 (20 mM HEPES, 10 mM triethanolamine, 150 mM NaCl, 10 mM CaCl<sub>2</sub>, 1 mM BME, 5% BSA, pH 8.0), wherein the BME was added fresh. Liposomal stocks were diluted 1:200 before incubation with cells such that the sDectin-2 protein concentration was 0.5  $\mu\text{g}/100 \mu\text{l}$ . After incubations of 15 min, 1-h, or longer, unbound liposomes washed out with 4 changes of LDB2. Merged images of rhodamine red fluorescent liposomes, green fluorescent cells, and differential interference contrast (DIC) illuminated cells were taken of cells grown on microscope slides under oil immersion at 63 $\times$  on a Leica DM6000B automated microscope. The DEC2-Rhod stock was also diluted 1:200 before incubation with cells such that the sDectin-2 protein concentration was also 0.5  $\mu\text{g}/100 \mu\text{l}$ . Bright-field, DIC, and red (excitation of 560 and emission of 645 [Ex560/Em645]) and green (Ex500/Em535) fluorescent images were taken of cells on microtiter plates at 20 $\times$  on an Olympus IX70 inverted microscope using an Olympus PEN E-PL7 digital camera, and the bright-field and/or fluorescent-colored layers were merged in Photoshop. The area of liposome binding at  $\times 20$  magnification was quantified by taking an 8-bit grayscale copy of the unmodified red fluorescent TIF image into Image J ([imagej.nih.gov/ij](http://imagej.nih.gov/ij)), using Image>Adjust>Threshold>Apply to capture just the red fluorescent areas illuminated by liposomes, and using Analyze>Measure to place the area data for each image in a file. Six to 10 photographic images were generally analyzed and averaged for most area estimates. However, because the staining intensities varied widely among photographic fields of *C. neoformans* cells, 90 images were analyzed for each treatment. Bright-field, DIC, and fluorescent images were also taken of cells grown in microscope chamber slides at 20 $\times$  or under oil immersion at 63 $\times$  on a Leica DM6000B automated microscope.

The glucuronoxylomannan (GXM)-specific monoclonal antibody 18B7 (60, 61) was obtained from Sigma-Aldrich (MABF2069), used at a 1:200 dilution (0.5  $\mu\text{g}/100 \mu\text{l}$ ), and visualized with secondary goat anti-mouse antibody Alexa 488 (Life Technologies, no. A11001) also diluted 1:200 and photographed with GFP filters (Ex500/Em535).

**Growth inhibition and viability assays following liposome treatment.** Liposomal stocks were stored at 615 to 800  $\mu\text{M}$  AmB and typically diluted first 30- to 600-fold into liposome dilution buffer, LDB2, and then diluted 1:11 into growth medium to achieve the indicated final fungicide concentrations ranging from 2  $\mu\text{M}$  down to 0.1  $\mu\text{M}$ . Control cells received an equivalent amount of LDB2. CellTiter-Blue (CTB) cell viability and metabolic activity assays of *C. albicans* and *A. fumigatus* were conducted as we recently described for *A. fumigatus*, by incubating cells with CTB reagent for 3 to 4 h (51) and analyzing 96-well plates in a Bio-Tek Synergy HT fluorescent microtiter plate reader. The fluorescent background from control wells was subtracted from experimental wells. Data from eight wells were averaged for each

data point. These assays had a lot of background and were less sensitive if the cells were assayed in VMM. We were unable to detect any fluorescent signal from CTB reagent when performing parallel cell viability assays on *C. neoformans* using this protocol or another CTB protocol published for this species (86). As an alternative measure of *C. neoformans* and *C. albicans* cell viability, assays were conducted by growing 1 ml of cells in YPD, adding drug-loaded liposomes for the indicated times of growth, diluting the cells, plating on YPD, and counting CFU. The fraction of dead *C. neoformans* cells among cells growing in YPD after treatment with fungicide-loaded liposomes was assayed by adding propidium iodide to the medium at 50  $\mu\text{g/ml}$  and incubating for 60 min at 37°C. The medium was removed and replaced with PBS for fluorescence microscopy using the red fluorescent protein channel (Ex560/Em595) and scoring the percentage of dead stained cells relative to the total number of stained and unstained cells. In experiments with DEC1-AmB-LLs, all liposomes were diluted with LDB1 (PBS plus 5% BSA plus 1 mM BME) (51) instead of LDB2.

## SUPPLEMENTAL MATERIAL

Supplemental material for this article may be found at <https://doi.org/10.1128/mSphere.00715-19>.

**FIG S1**, JPG file, 0.5 MB.

**FIG S2**, JPG file, 0.7 MB.

**FIG S3**, JPG file, 0.2 MB.

**FIG S4**, JPG file, 0.3 MB.

**FIG S5**, JPG file, 0.8 MB.

**FIG S6**, JPG file, 0.6 MB.

**TABLE S1**, XLSX file, 0.1 MB.

## ACKNOWLEDGMENTS

We thank our University of Georgia colleagues Zachary Wood for instructive discussions concerning the purification of sDectin-2, Bradley Phillips for discussions of the current problems concerning the clinical treatment of invasive fungal diseases, Walter K. Schmitz and Brittany M. Berger for assistance with a fluorescent microtiter plate reader, Michelle Momany and S. Earl Kang for providing the *A. fumigatus* strain, and James Konopka from Stony Brook University for his gift of the GFP fluorescent *C. albicans* strain.

Funding was provided as follows: to S.A., E.C.E., and R.B.M. from the University of Georgia Research Foundation, Inc., UGARF, NIAID R21 AI144498, NIH National Center for Advancing Translational Sciences no. UL1TR002378; to Z.A.L. from American Cancer Society RSG-14-184-01-DMC and from NIGMS R01GM132644; and to X.L. from NIAID 1R01AI140719. None of the authors have any financial conflicts of interest.

## REFERENCES

- Bongomin F, Gago S, Oladele RO, Denning DW. 2017. Global and multi-national prevalence of fungal diseases-estimate precision. *J Fungi (Basel)* 3. <https://doi.org/10.3390/jof3040057>.
- CDC. 2018. Fungal diseases. <https://www.cdc.gov/fungal/index.html>.
- Low CY, Rotstein C. 2011. Emerging fungal infections in immunocompromised patients. *F1000 Med Rep* 3:14. <https://doi.org/10.3410/M3-14>.
- Taylor P. 2017. Antifungal drugs: technologies and global markets. Research B, Wellesley, MA.
- Brown GD, Denning DW, Gow NA, Levitz SM, Netea MG, White TC. 2012. Hidden killers: human fungal infections. *Sci Transl Med* 4:165rv113. <https://doi.org/10.1126/scitranslmed.3004404>.
- Benedict K, Jackson BR, Chiller T, Beer KD. 2019. Estimation of direct healthcare costs of fungal diseases in the United States. *Clin Infect Dis* 68:1791–1797. <https://doi.org/10.1093/cid/ciy776>.
- Zaoutis TE, Heydon K, Chu JH, Walsh TJ, Steinbach WJ. 2006. Epidemiology, outcomes, and costs of invasive aspergillosis in immunocompromised children in the United States, 2000. *Pediatrics* 117:e711–e716. <https://doi.org/10.1542/peds.2005-1161>.
- Denning DW, Pleuvry A, Cole DC. 2011. Global burden of chronic pulmonary aspergillosis as a sequel to pulmonary tuberculosis. *Bull World Health Organ* 89:864–872. <https://doi.org/10.2471/BLT.11.089441>.
- Whitney LC, Bicanic T. 2015. Treatment principles for *Candida* and *Cryptococcus*. *Cold Spring Harb Perspect Med* 5:a024158. <https://doi.org/10.1101/cshperspect.a024158>.
- Allen U. 2010. Antifungal agents for the treatment of systemic fungal infections in children. *Paediatr Child Health* 15:603–608.
- Dupont B. 2002. Overview of the lipid formulations of amphotericin B. *J Antimicrob Chemother* 49(Suppl 1):31–36. [https://doi.org/10.1093/jac/49.suppl\\_1.31](https://doi.org/10.1093/jac/49.suppl_1.31).
- Tonin FS, Steimbach LM, Borba HH, Sanches AC, Wiens A, Pontarolo R, Fernandez-Llimos F. 2017. Efficacy and safety of amphotericin B formulations: a network meta-analysis and a multicriteria decision analysis. *J Pharm Pharmacol* 69:1672–1683. <https://doi.org/10.1111/jphp.12802>.
- Chastain DB, Giles RL, Bland CM, Franco-Paredes C, Henaó-Martínez AF, Young HN. 2019. A clinical pharmacist survey of prophylactic strategies used to prevent adverse events of lipid-associated formulations of amphotericin B. *Infect Dis (Lond)* 51:380–383. <https://doi.org/10.1080/23744235.2019.1568546>.
- Sanguinetti M, Posteraro B, Lass-Flörl C. 2015. Antifungal drug resistance among *Candida* species: mechanisms and clinical impact. *Mycoses* 58(Suppl 2):2–13. <https://doi.org/10.1111/myc.12330>.
- Smith KD, Achan B, Hullsiek KH, McDonald TR, Okagaki LH, Alhadab AA, Akampurira A, Rhein JR, Meya DB, Boulware DR, Nielsen K, Team A-C. 2015. Increased antifungal drug resistance in clinical isolates of *Cryptococcus neoformans* in Uganda. *Antimicrob Agents Chemother* 59:7197–7204. <https://doi.org/10.1128/AAC.01299-15>.
- Jensen RH. 2016. Resistance in human pathogenic yeasts and filamentous fungi: prevalence, underlying molecular mechanisms and link to

- the use of antifungals in humans and the environment. *Dan Med J* 63:1–34.
17. Tashiro M, Izumikawa K. 2016. The current status of drug-resistant *Aspergillus*. *Med Mycol J* 57:J103–J112. <https://doi.org/10.3314/mmj.16.001>.
  18. Aigner M, Lass-Flörl C. 2015. Treatment of drug-resistant *Aspergillus* infection. *Expert Opin Pharmacother* 16:2267–2270. <https://doi.org/10.1517/14656566.2015.1083976>.
  19. Perfect JR. 2017. The antifungal pipeline: a reality check. *Nat Rev Drug Discov* 16:603–616. <https://doi.org/10.1038/nrd.2017.46>.
  20. Warn PA, Sharp A, Denning DW. 2006. In vitro activity of a new triazole BAL4815, the active component of BAL8557 (the water-soluble prodrug), against *Aspergillus* spp. *J Antimicrob Chemother* 57:135–138. <https://doi.org/10.1093/jac/dki399>.
  21. Odds FC. 2006. Drug evaluation: BAL-8557—a novel broad-spectrum triazole antifungal. *Curr Opin Invest Drugs* 7:766–772.
  22. Huang A, Kennel SJ, Huang L. 1983. Interactions of immunoliposomes with target cells. *J Biol Chem* 258:14034–14040.
  23. Connor J, Huang L. 1986. pH-sensitive immunoliposomes as an efficient and target-specific carrier for antitumor drugs. *Cancer Res* 46:3431–3435.
  24. Paul JW, Hua S, Ilicic M, Tolosa JM, Butler T, Smith R. 2017. Drug delivery to the human and mouse uterus using immunoliposomes targeted to the oxytocin receptor. *Am J Obstet Gynecol* 216:283.e1–283.e14. <https://doi.org/10.1016/j.ajog.2016.08.027>.
  25. Mamot C, Drummond DC, Noble CO, Kallab V, Guo Z, Hong K, Kirpotin DB, Park JW. 2005. Epidermal growth factor receptor-targeted immunoliposomes significantly enhance the efficacy of multiple anticancer drugs in vivo. *Cancer Res* 65:11631–11638. <https://doi.org/10.1158/0008-5472.CAN-05-1093>.
  26. Koren E, Apte A, Jani A, Torchilin VP. 2012. Multifunctional PEGylated 2C5-immunoliposomes containing pH-sensitive bonds and TAT peptide for enhanced tumor cell internalization and cytotoxicity. *J Control Release* 160:264–273. <https://doi.org/10.1016/j.jconrel.2011.12.002>.
  27. Shi J, Kantoff PW, Wooster R, Farokhzad OC. 2017. Cancer nanomedicine: progress, challenges and opportunities. *Nat Rev Cancer* 17:20–37. <https://doi.org/10.1038/nrc.2016.108>.
  28. Allen TM. 2002. Ligand-targeted therapeutics in anticancer therapy. *Nat Rev Cancer* 2:750–763. <https://doi.org/10.1038/nrc903>.
  29. Fan Y, Zhang Q. 2013. Development of liposomal formulations: from concept to clinical investigations. *Asian J Pharm Sci* 8:81–87. <https://doi.org/10.1016/j.ajps.2013.07.010>.
  30. Ait-Oudhia S, Mager DE, Straubinger RM. 2014. Application of pharmacokinetic and pharmacodynamic analysis to the development of liposomal formulations for oncology. *Pharmaceutics* 6:137–174. <https://doi.org/10.3390/pharmaceutics6010137>.
  31. Eloy JO, Petrilli R, Trevizan LNF, Chorilli M. 2017. Immunoliposomes: a review on functionalization strategies and targets for drug delivery. *Colloids Surf B Biointerfaces* 159:454–467. <https://doi.org/10.1016/j.colsurfb.2017.07.085>.
  32. Chandra J, Mukherjee PK, Ghannoum MA. 2012. *Candida* biofilms associated with CVC and medical devices. *Mycoses* 55:46–57. <https://doi.org/10.1111/j.1439-0507.2011.02149.x>.
  33. Mathe L, Van Dijck P. 2013. Recent insights into *Candida albicans* biofilm resistance mechanisms. *Curr Genet* 59:251–264. <https://doi.org/10.1007/s00294-013-0400-3>.
  34. Martinez LR, Casadevall A. 2015. Biofilm formation by *Cryptococcus neoformans*. *Microbiol Spectr* 3. <https://doi.org/10.1128/microbiolspec.MB-0006-2014>.
  35. Yang M, Du K, Hou Y, Xie S, Dong Y, Li D, Du Y. 2019. Synergistic antifungal effect of amphotericin B-loaded poly(lactic-co-glycolic acid) nanoparticles and ultrasound against *Candida albicans* biofilms. *Antimicrob Agents Chemother* 63:e02022-18. <https://doi.org/10.1128/AAC.02022-18>.
  36. Escande W, Fayad G, Modine T, Verbrugge E, Koussa M, Senneville E, Leroy O. 2011. Culture of a prosthetic valve excised for streptococcal endocarditis positive for *Aspergillus fumigatus* 20 years after previous *A. fumigatus* endocarditis. *Ann Thorac Surg* 91:e92–e93. <https://doi.org/10.1016/j.athoracsur.2011.01.102>.
  37. Tan Y, Ma S, Leonhard M, Moser D, Schneider-Stickler B. 2018. Beta-1,3-galactanase disrupts biofilm formation and increases antifungal susceptibility of *Candida albicans* DAY185. *Int J Biol Macromol* 108:942–946. <https://doi.org/10.1016/j.ijbiomac.2017.11.003>.
  38. Korem M, Kagan S, Polachek I. 2017. The effect of novel heterocyclic compounds on cryptococcal biofilm. *J Fungi (Basel)* 3. <https://doi.org/10.3390/jof3030042>.
  39. Al-Fattani MA, Douglas LJ. 2006. Biofilm matrix of *Candida albicans* and *Candida tropicalis*: chemical composition and role in drug resistance. *J Med Microbiol* 55:999–1008. <https://doi.org/10.1099/jmm.0.46569-0>.
  40. Mukherjee PK, Chandra J. 2004. *Candida* biofilm resistance. *Drug Resist Updat* 7:301–309. <https://doi.org/10.1016/j.drug.2004.09.002>.
  41. Taff HT, Mitchell KF, Edward JA, Andes DR. 2013. Mechanisms of *Candida* biofilm drug resistance. *Future Microbiol* 8:1325–1337. <https://doi.org/10.2217/fmb.13.101>.
  42. Ishikawa T, Itoh F, Yoshida S, Saijo S, Matsuzawa T, Gono T, Saito T, Okawa Y, Shibata N, Miyamoto T, Yamasaki S. 2013. Identification of distinct ligands for the C-type lectin receptors Mincle and Dectin-2 in the pathogenic fungus *Malassezia*. *Cell Host Microbe* 13:477–488. <https://doi.org/10.1016/j.chom.2013.03.008>.
  43. Hollmig ST, Ariizumi K, Cruz PD. Jr., 2009. Recognition of non-self-polysaccharides by C-type lectin receptors dectin-1 and dectin-2. *Glycobiology* 19:568–575. <https://doi.org/10.1093/glycob/cwp032>.
  44. McGreal EP, Rosas M, Brown GD, Zamze S, Wong SY, Gordon S, Martinez-Pomares T, Taylor PR. 2006. The carbohydrate-recognition domain of Dectin-2 is a C-type lectin with specificity for high mannose. *Glycobiology* 16:422–430. <https://doi.org/10.1093/glycob/cwj077>.
  45. Saijo S, Ikeda S, Yamabe K, Kakuta S, Ishigame H, Akitsu A, Fujikado N, Kusaka T, Kubo S, Chung SH, Komatsu R, Miura N, Adachi Y, Ohno N, Shibuya K, Yamamoto N, Kawakami K, Yamasaki S, Saito T, Akira S, Iwakura Y. 2010. Dectin-2 recognition of alpha-mannans and induction of Th17 cell differentiation is essential for host defense against *Candida albicans*. *Immunity* 32:681–691. <https://doi.org/10.1016/j.immuni.2010.05.001>.
  46. Hirata N, Ishibashi K, Sato W, Nagi-Miura N, Adachi Y, Ohta S, Ohno N. 2013. Beta-mannosyl linkages inhibit CAWS arteritis by negatively regulating dectin-2-dependent signaling in spleen and dendritic cells. *Immunopharmacol Immunotoxicol* 35:594–604. <https://doi.org/10.3109/08923973.2013.830124>.
  47. Sato K, Yang XL, Yudate T, Chung JS, Wu J, Luby-Phelps K, Kimberly RP, Underhill D, Cruz PD, Jr, Ariizumi K. 2006. Dectin-2 is a pattern recognition receptor for fungi that couples with the Fc receptor gamma chain to induce innate immune responses. *J Biol Chem* 281:38854–38866. <https://doi.org/10.1074/jbc.M606542200>.
  48. Zhu LL, Zhao XQ, Jiang C, You Y, Chen XP, Jiang YY, Jia XM, Lin X. 2013. C-type lectin receptors Dectin-3 and Dectin-2 form a heterodimeric pattern-recognition receptor for host defense against fungal infection. *Immunity* 39:324–334. <https://doi.org/10.1016/j.immuni.2013.05.017>.
  49. Ifrim DC, Quintin J, Courjol F, Verschueren I, van Krieken JH, Koentgen F, Fradin C, Gow NA, Joosten LA, van der Meer JW, van de Veerdonk F, Netea MG. 2016. The role of Dectin-2 for host defense against disseminated candidiasis. *J Interferon Cytokine Res* 36:267–276. <https://doi.org/10.1089/jir.2015.0040>.
  50. Brown BR, Lee EJ, Snow PE, Vance EE, Iwakura Y, Ohno N, Miura N, Lin X, Brown GD, Wells CA, Smith JR, Caspi RR, Rosenzweig HL. 2017. Fungal-derived cues promote ocular autoimmunity through a Dectin-2/Card9-mediated mechanism. *Clin Exp Immunol* 190:293–303. <https://doi.org/10.1111/cei.13021>.
  51. Ambati S, Ferraro AR, Kang SE, Lin J, Lin X, Momany M, Lewis ZA, Meagher RB. 2019. Dectin-1-targeted antifungal liposomes exhibit enhanced efficacy. *mSphere* 4:e00025-19. <https://doi.org/10.1128/mSphere.00121-19>.
  52. Gantner BN, Simmons RM, Underhill DM. 2005. Dectin-1 mediates macrophage recognition of *Candida albicans* yeast but not filaments. *EMBO J* 24:1277–1286. <https://doi.org/10.1038/sj.emboj.7600594>.
  53. Heinsbroek SE, Brown GD, Gordon S. 2005. Dectin-1 escape by fungal dimorphism. *Trends Immunol* 26:352–354. <https://doi.org/10.1016/j.it.2005.05.005>.
  54. Wheeler RT, Kombe D, Agarwala SD, Fink GR. 2008. Dynamic, morphotype-specific *Candida albicans* beta-glucan exposure during infection and drug treatment. *PLoS Pathog* 4:e1000227. <https://doi.org/10.1371/journal.ppat.1000227>.
  55. Bain JM, Louw J, Lewis LE, Okai B, Walls CA, Ballou ER, Walker LA, Reid D, Munro CA, Brown AJ, Brown GD, Gow NA, Erwig LP. 2014. *Candida albicans* hypha formation and mannann masking of  $\beta$ -glucan inhibit macrophage phagosome maturation. *mBio* 5:e01874. <https://doi.org/10.1128/mBio.01874-14>.
  56. Davis SE, Hopke A, Minkin SC, Jr, Montedonico AE, Wheeler RT, Reynolds TB. 2014. Masking of  $\beta(1-3)$ -glucan in the cell wall of *Candida albicans*

- from detection by innate immune cells depends on phosphatidylserine. *Infect Immun* 82:4405–4413. <https://doi.org/10.1128/IAI.01612-14>.
57. Gilead Sciences. March 2012. AmBisome (Amphotericin B) liposome for injection. [https://www.gilead.com/-/media/files/pdfs/medicines/other/ambisome/ambisome\\_pi.pdf](https://www.gilead.com/-/media/files/pdfs/medicines/other/ambisome/ambisome_pi.pdf).
  58. Stone NR, Bicanic T, Salim R, Hope W. 2016. Liposomal amphotericin B (AmBisome®): a review of the pharmacokinetics, pharmacodynamics, clinical experience and future directions. *Drugs* 76:485–500. <https://doi.org/10.1007/s40265-016-0538-7>.
  59. Adler-Moore JP, Proffitt RT. 2008. Amphotericin B lipid preparations: what are the differences? *Clin Microbiol Infect* 14(Suppl 4):25–36. <https://doi.org/10.1111/j.1469-0691.2008.01979.x>.
  60. Casadevall A, Cleare W, Feldmesser M, Glatman-Freedman A, Goldman DL, Kozel TR, Lendvai N, Mukherjee J, Pirofski LA, Rivera J, Rosas AL, Scharff MD, Valadon P, Westin K, Zhong Z. 1998. Characterization of a murine monoclonal antibody to *Cryptococcus neoformans* polysaccharide that is a candidate for human therapeutic studies. *Antimicrob Agents Chemother* 42:1437–1446. <https://doi.org/10.1128/AAC.42.6.1437>.
  61. Martinez LR, Casadevall A. 2005. Specific antibody can prevent fungal biofilm formation and this effect correlates with protective efficacy. *Infect Immun* 73:6350–6362. <https://doi.org/10.1128/IAI.73.10.6350-6362.2005>.
  62. Erickson HP. 2009. Size and shape of protein molecules at the nanometer level determined by sedimentation, gel filtration, and electron microscopy. *Biol Proced Online* 11:32–51. <https://doi.org/10.1007/s12575-009-9008-x>.
  63. Barchiesi F, Schimizzi AM, Caselli F, Novelli A, Fallani S, Giannini D, Arzeni D, Di Cesare S, Di Francesco LF, Fortuna M, Giacometti A, Carle F, Mazzei T, Scalise G. 2000. Interactions between triazoles and amphotericin B against *Cryptococcus neoformans*. *Antimicrob Agents Chemother* 44:2435–2441. <https://doi.org/10.1128/aac.44.9.2435-2441.2000>.
  64. de Aquino Lemos J, Costa CR, de Araújo CR, Souza LKHE, Silva M. d R R. 2009. Susceptibility testing of *Candida albicans* isolated from oropharyngeal mucosa of HIV(+) patients to fluconazole, amphotericin B and caspofungin. Killing kinetics of caspofungin and amphotericin B against fluconazole resistant and susceptible isolates. *Braz J Microbiol* 40:163–169. <https://doi.org/10.1590/S1517-838220090001000028>.
  65. Borman AM, Fraser M, Palmer MD, Szekely A, Houldsworth M, Patterson Z, Johnson EM. 2017. MIC distributions and evaluation of fungicidal activity for amphotericin B, itraconazole, voriconazole, posaconazole and caspofungin and 20 species of pathogenic filamentous fungi determined using the CLSI broth microdilution method. *J Fungi (Basel)* 3. <https://doi.org/10.3390/jof3020027>.
  66. Ryder NS, Leitner I. 2001. Synergistic interaction of terbinafine with triazoles or amphotericin B against *Aspergillus* species. *Med Mycol* 39:91–95. <https://doi.org/10.1080/mmy.39.1.91.95>.
  67. Davis SA, Vincent BM, Endo MM, Whitesell L, Marchillo K, Andes DR, Lindquist S, Burke MD. 2015. Nontoxic antimicrobials that evade drug resistance. *Nat Chem Biol* 11:481–487. <https://doi.org/10.1038/nchembio.1821>.
  68. Feinberg H, Jegouzo SAF, Rex MJ, Drickamer K, Weis WI, Taylor ME. 2017. Mechanism of pathogen recognition by human Dectin-2. *J Biol Chem* 292:13402–13414. <https://doi.org/10.1074/jbc.M117.799080>.
  69. Adams EL, Rice PJ, Graves B, Ensley HE, Yu H, Brown GD, Gordon S, Monteiro MA, Papp-Szabo E, Lowman DW, Power TD, Wempe MF, Williams DL. 2008. Differential high-affinity interaction of dectin-1 with natural or synthetic glucans is dependent upon primary structure and is influenced by polymer chain length and side-chain branching. *J Pharmacol Exp Ther* 325:115–123. <https://doi.org/10.1124/jpet.107.133124>.
  70. Dominguez E, Zarnowski R, Sanchez H, Covelli AS, Westler WM, Azadi P, Nett J, Mitchell AP, Andes DR. 2018. Conservation and divergence in the *Candida* species biofilm matrix mannan-glucan complex structure, function, and genetic control. *mBio* 9:e00451-18. <https://doi.org/10.1128/mBio.00451-18>.
  71. Vaishnav VV, Bacon BE, O'Neill M, Cherniak R. 1998. Structural characterization of the galactoxylomannan of *Cryptococcus neoformans* Cap67. *Carbohydr Res* 306:315–330. [https://doi.org/10.1016/S0008-6215\(97\)10058-1](https://doi.org/10.1016/S0008-6215(97)10058-1).
  72. Beauvais A, Latge JP. 2015. *Aspergillus* biofilm in vitro and in vivo. *Microbiol Spectr* 3. <https://doi.org/10.1128/microbiolspec.MB-0017-2015>.
  73. Beauvais A, Fontaine T, Aimaiana V, Latge JP. 2014. *Aspergillus* cell wall and biofilm. *Mycopathologia* 178:371–377. <https://doi.org/10.1007/s11046-014-9766-0>.
  74. Zarnowski R, Westler WM, Lacmouh GA, Marita JM, Bothe JR, Bernhardt J, Lounes-Hadj Sahraoui A, Fontaine J, Sanchez H, Hatfield RD, Ntambi JM, Nett JE, Mitchell AP, Andes DR. 2014. Novel entries in a fungal biofilm matrix encyclopedia. *mBio* 5:e01333. <https://doi.org/10.1128/mBio.01333-14>.
  75. Vecchiarelli A, Pericolini E, Gabrielli E, Chow SK, Bistoni F, Cenci E, Casadevall A. 2011. *Cryptococcus neoformans* galactoxylomannan is a potent negative immunomodulator, inspiring new approaches in anti-inflammatory immunotherapy. *Immunotherapy* 3:997–1005. <https://doi.org/10.2217/imt.11.86>.
  76. Martinez LR, Casadevall A. 2007. *Cryptococcus neoformans* biofilm formation depends on surface support and carbon source and reduces fungal cell susceptibility to heat, cold, and UV light. *Appl Environ Microbiol* 73:4592–4601. <https://doi.org/10.1128/AEM.02506-06>.
  77. Beauvais A, Schmidt C, Guadagnini S, Roux P, Perret E, Henry C, Paris S, Mallet A, Prevost MC, Latge JP. 2007. An extracellular matrix glues together the aerial-grown hyphae of *Aspergillus fumigatus*. *Cell Microbiol* 9:1588–1600. <https://doi.org/10.1111/j.1462-5822.2007.00895.x>.
  78. Esher SK, Ost KS, Kohlbrenner MA, Pianalto KM, Telzrow CL, Campuzano A, Nichols CB, Munro C, Wormley FL, Jr, Alspaugh JA. 2018. Defects in intracellular trafficking of fungal cell wall synthases lead to aberrant host immune recognition. *PLoS Pathog* 14:e1007126. <https://doi.org/10.1371/journal.ppat.1007126>.
  79. Schiavone M, Vax A, Formosa C, Martin-Yken H, Dague E, François JM. 2014. A combined chemical and enzymatic method to determine quantitatively the polysaccharide components in the cell wall of yeasts. *FEMS Yeast Res* 14:933–947. <https://doi.org/10.1111/1567-1364.12182>.
  80. Shi QY, Camara CRS, Schlegel V. 2018. Biochemical alterations of *Candida albicans* during the phenotypic transition from yeast to hyphae captured by Fourier transform mid-infrared-attenuated reflectance spectroscopy. *Analyst* 143:5404–5416. <https://doi.org/10.1039/c8an01452c>.
  81. Kuramae EE, Robert V, Snel B, Weiss M, Boekhout T. 2006. Phylogenomics reveal a robust fungal tree of life. *FEMS Yeast Res* 6:1213–1220. <https://doi.org/10.1111/j.1567-1364.2006.00119.x>.
  82. Padovan AC, Sanson GF, Brunstein A, Briones MR. 2005. Fungi evolution revisited: application of the penalized likelihood method to a Bayesian fungal phylogeny provides a new perspective on phylogenetic relationships and divergence dates of Ascomycota groups. *J Mol Evol* 60:726–735. <https://doi.org/10.1007/s00239-004-0164-y>.
  83. Keppeler-Ross S, Douglas L, Konopka JB, Dean N. 2010. Recognition of yeast by murine macrophages requires mannan but not glucan. *Eukaryot Cell* 9:1776–1787. <https://doi.org/10.1128/EC.00156-10>.
  84. Montone KT. 2009. Regulating the T-cell immune response toward the H99 strain of *Cryptococcus neoformans*. *Am J Pathol* 175:2255–2256. <https://doi.org/10.2353/ajpath.2009.090891>.
  85. Vogel HJ. 1956. A convenient growth medium for *Neurospora crassa*. *Microb Genet Bull* 32:42–43.
  86. Rabjohns JLA, Park YD, Dehdashti J, Henderson C, Zelazny A, Metallo SJ, Zheng W, Williamson PR. 2014. A high-throughput screening assay for fungicidal compounds against *Cryptococcus neoformans*. *J Biomol Screen* 19:270–277. <https://doi.org/10.1177/1087057113496847>.
  87. Alberts B, Johnson A, Lewis J, Raff M, Roberts K, Walter P. 2008. *Molecular biology of the cell*, 5th ed, p 1539–1600. Garland Science, Taylor and Francis Group, USA, Boca Raton, FL.
  88. Hamill RJ. 2013. Amphotericin B formulations: a comparative review of efficacy and toxicity. *Drugs* 73:919–934. <https://doi.org/10.1007/s40265-013-0069-4>.
  89. Gaboriau F, Cheron M, Petit C, Bolard J. 1997. Heat-induced superaggregation of amphotericin B reduces its in vitro toxicity: a new way to improve its therapeutic index. *Antimicrob Agents Chemother* 41:2345–2351. <https://doi.org/10.1128/AAC.41.11.2345>.